CrossMark

Solution of the Adiabatic Sound Wave Equation as a Nonlinear Least Squares Problem

Muhamed Bijedić[1] · Sabina Begić[1]

Abstract

A new method for deriving accurate thermodynamic properties of gases and vapors (the compression factor and heat capacities) from the speed of sound is recommended. A set of PDEs connecting speed of sound with other thermodynamic properties is solved as a nonlinear least squares problem, using a modified Levenberg–Marquardt algorithm. In supercritical domain, boundary values of compression factor are imposed along two isotherms (one slightly above T_c and another several times T_c) and two isochores (one at zero density and another slightly above ρ_c). In subcritical domain, the upper isochore is replaced by the saturation line, the lower isotherm is slightly above the triple point, and the upper isotherm is slightly below the critical point. Initial values of compression factor inside the domains are obtained from the boundary values by a cubic spline interpolation with respect to density. All the partial derivation with respect to density and temperature, as well as speed of sound interpolation with respect to pressure, is also conducted by a cubic spline. The method is tested with Ar, CH_4 and CO_2. The average absolute deviation of compression factor and heat capacities is better than 0.002 % and 0.1 %, respectively.

Keywords Density · Heat capacity · Least squares · Levenberg–Marquardt · Speed of sound

---

✉ Muhamed Bijedić
muhamed.bijedic@untz.ba

Sabina Begić
sabina.begic@untz.ba

[1] Department of Chemical Engineering, Faculty of Technology, University of Tuzla, Univerzitetska 8, 75000 Tuzla, Bosnia and Herzegovina

1 Introduction

The speed of sound is an intensive property whose value depends on the state of the medium through which sound propagates [1]. Nowadays, speed of sound is measured with exceptional accuracy and represents potential source of other (thermodynamic) properties which are measured less accurately. However, in order to derive any other property of the medium from the speed of sound it is necessary to solve a set of nonlinear partial differential equations (PDEs) of the second order [2]. Instead of seeking for a general solution, some researchers suggest various methods of numerical integration for obtaining a particular solution [3–10]. A method which covers a wider domain of solutions, with a fewer and less demanding initial/boundary conditions, may be considered more superior. For example, initial/boundary conditions of Dirichlet type are less demanding than those of Neumann type. Similarly, those composed of volumetric properties (density, compression factor) are less demanding than the ones composed of caloric properties (heat capacity). Therefore, a method using only volumetric initial/boundary conditions of Dirichlet type is desirable. Although the problem is not solvable by numerical integration using only volumetric initial conditions of Dirichlet type, it can be solved using only volumetric boundary conditions of Dirichlet type [11]. However, this approach is not based on numerical integration but rather on discretization. Namely, the set of PDEs is converted into the set of nonlinear algebraic equations by approximating all the derivatives by finite differences. The main disadvantage of this approach is rather huge number of equations (of the order 10^4). In this paper, an approach based on a cubic spline [12] is used to decrease the number of equations, which are solved as a nonlinear least squares problem by a modified Levenberg–Marquardt algorithm [13–15]. Since the values of thermodynamic properties are only locally represented by cubic polynomials, there is no analytical equation of state.

2 Theory

The adiabatic sound wave equation [1]

$$u^2 = \left(\frac{\partial p}{\partial \rho}\right)_s \tag{1}$$

connects the speed of sound u with thermodynamic properties of a medium through which the wave propagates (p is the pressure, ρ is the density, and s is specific entropy).

Since entropy is not measurable quantity, it can be avoided with the help of the following relation [1]

$$\left(\frac{\partial p}{\partial \rho}\right)_s = \frac{c_p}{c_v}\left(\frac{\partial p}{\partial \rho}\right)_T \tag{2}$$

where T is the temperature, c_p is specific heat capacity at constant pressure and c_v is specific heat capacity at constant volume.

Combining (1) and (2), one obtains

$$u^2 = \frac{c_p}{c_v}\left(\frac{\partial p}{\partial \rho}\right)_T \tag{3}$$

If c_p in (3) is replaced by [1]

$$c_p = c_v + \frac{T}{\rho^2}\left(\frac{\partial p}{\partial \rho}\right)_T^{-1}\left(\frac{\partial p}{\partial T}\right)_\rho^2 \tag{4}$$

one obtains

$$u^2 = \left(\frac{\partial p}{\partial \rho}\right)_T + \frac{T}{\rho^2 c_v}\left(\frac{\partial p}{\partial T}\right)_\rho^2 \tag{5}$$

If pressure in (5) is replaced by a less varying compression factor

$$Z = \frac{pM}{\rho RT} \tag{6}$$

where M is the molar mass and R is the universal gas constant, after rearrangement one obtains

$$c_v = \frac{R}{M}\left[Z + T\left(\frac{\partial Z}{\partial T}\right)_\rho\right]^2\left[\frac{Mu^2}{RT} - Z - \rho\left(\frac{\partial Z}{\partial \rho}\right)_T\right]^{-1} \tag{7}$$

If (7) is coupled with [16]

$$\left(\frac{\partial c_v}{\partial \rho}\right)_T = -\frac{T}{\rho^2}\left(\frac{\partial^2 p}{\partial T^2}\right)_\rho \tag{8}$$

(3), (7) and (8) may be solved for Z, c_v and c_p in a rectangular ρ–T domain (supercritical region), respectively. To perform that the values of c_v obtained from (7) are partially derived with respect to density, at constant temperature, by a cubic spline. Then, these derivatives are calculated again, but this time from (8). The function which quantifies difference between derivatives obtained in these two different ways is

$$f = -\frac{T}{\rho^2}\left(\frac{\partial^2 p}{\partial T^2}\right)_\rho - \left(\frac{\partial c_v}{\partial \rho}\right)_T \tag{9}$$

Finally, the objective function is calculated according to

$$g = \frac{1}{2}\sum f^2 \tag{10}$$

The aim is to find such values of Z which minimize objective function g. Since functions f are nonlinear with respect to Z, this problem may be solved as a nonlinear least squares problem using a modified Levenberg–Marquardt algorithm.

If p in (8) is replaced by Z, one obtains

$$\left(\frac{\partial c_v}{\partial \rho}\right)_T = -\frac{RT}{M\rho}\left[2\left(\frac{\partial Z}{\partial T}\right)_\rho + T\left(\frac{\partial^2 Z}{\partial T^2}\right)_\rho\right] \tag{11}$$

If a new variable is introduced

$$\phi = \frac{\rho}{\rho_{sat}} \tag{12}$$

where ρ_{sat} is density of saturated vapor at a given temperature, then, according to calculus,

$$\left(\frac{\partial Z}{\partial T}\right)_\rho = \left(\frac{\partial Z}{\partial T}\right)_\phi - \left(\frac{\partial Z}{\partial \rho}\right)_T\left(\frac{\partial \rho}{\partial T}\right)_\phi \tag{13}$$

and

$$\left(\frac{\partial^2 Z}{\partial T^2}\right)_\rho = \left[\frac{\partial}{\partial T}\left(\frac{\partial Z}{\partial T}\right)_\rho\right]_\phi - \frac{\partial^2 Z}{\partial T \partial \rho}\left(\frac{\partial \rho}{\partial T}\right)_\phi \tag{14}$$

So, (7) and (11) become

$$c_v = \frac{R}{M}\left\{Z + T\left[\left(\frac{\partial Z}{\partial T}\right)_\phi - \left(\frac{\partial Z}{\partial \rho}\right)_T\left(\frac{\partial \rho}{\partial T}\right)_\phi\right]\right\}^2\left[\frac{Mu^2}{RT} - Z - \rho\left(\frac{\partial Z}{\partial \rho}\right)_T\right]^{-1} \tag{15}$$

and

$$\left(\frac{\partial c_v}{\partial \rho}\right)_T = -\frac{RT}{M\rho}\left\{2\left[\left(\frac{\partial Z}{\partial T}\right)_\phi - \left(\frac{\partial Z}{\partial \rho}\right)_T\left(\frac{\partial \rho}{\partial T}\right)_\phi\right]\right.$$
$$\left. + T\left\{\left[\frac{\partial}{\partial T}\left(\frac{\partial Z}{\partial T}\right)_\rho\right]_\phi - \frac{\partial^2 Z}{\partial T \partial \rho}\left(\frac{\partial \rho}{\partial T}\right)_\phi\right\}\right\} \tag{16}$$

respectively. Now, (3), (15) and (16) may be solved for Z, c_v and c_p in a rectangular ϕ–T domain (subcritical region), respectively. The procedure of solution is the same as the one described for the supercritical region, with

$$f = -\frac{RT}{M\rho}\left\{2\left[\left(\frac{\partial Z}{\partial T}\right)_\phi - \left(\frac{\partial Z}{\partial \rho}\right)_T\left(\frac{\partial \rho}{\partial T}\right)_\phi\right]\right.$$
$$\left. + T\left\{\left[\frac{\partial}{\partial T}\left(\frac{\partial Z}{\partial T}\right)_\rho\right]_\phi - \frac{\partial^2 Z}{\partial T \partial \rho}\left(\frac{\partial \rho}{\partial T}\right)_\phi\right\}\right\} - \left(\frac{\partial c_v}{\partial \rho}\right)_T \tag{17}$$

and

$$g = \frac{1}{2} \sum f^2 \tag{18}$$

2.1 Supercritical Domain

This domain is bounded by two isotherms and two isochores. It is practical, but not necessary, that the lower isochore is in the limit of ideal gas, because along this isochore the compression factor has unique value 1, and the heat capacities are obtained from speed of sound measurements (extrapolated to zero pressure) directly. The temperature and density ranges are divided into several isotherms and several isochores, respectively. Pressures are calculated along each isochore from the Peng–Robinson equation of state [17], and speed of sound values [18–20] are specified at these pressures in the form of a less varying quantity $F = Mu^2/(RT)$, which is more suitable for interpolation. Several data points of compression factor [18–20] are specified along the boundary of the domain. Initial values of compression factor inside the domain are obtained from these boundary values, by a cubic spline interpolation with respect to density.

2.1.1 Algorithm of Solution

1. For the specified set of isotherms and isochores, pressures inside the domain ($T_{min} < T < T_{max}$ and $\rho_{min} < \rho < \rho_{max}$) are calculated from compression factors, since they are always known in advance in each iteration. (In the first iteration they are obtained from the boundary values and in all other iterations from a modified Levenberg–Marquardt algorithm.) In any case, this is done by rewriting (6) into

$$p = \frac{\rho R T Z}{M}$$

2. Having calculated pressures at different temperatures along each isochore inside the domain, with boundary pressures fixed at their specified values all the time, partial derivatives

$$\left(\partial p / \partial T \right)_\rho$$

are estimated from a cubic spline, inside the domain and along the boundary ($T_{min} \leq T \leq T_{max}$ and $\rho_{min} < \rho \leq \rho_{max}$), except along $\rho = \rho_{min}$, since

$$\left(\frac{\partial p}{\partial T} \right)_{\rho_{min}=0} = 0$$

3. Partial derivatives of compression factor, with respect to temperature at constant density, are calculated directly from the following relation

$$\left(\frac{\partial Z}{\partial T} \right)_\rho = \frac{M}{\rho R T} \left[\left(\frac{\partial p}{\partial T} \right)_\rho - \frac{p}{T} \right]$$

which is obtained by analytical derivation of (6), inside the domain and along the boundary ($T_{\min} \leq T \leq T_{\max}$ and $\rho_{\min} < \rho \leq \rho_{\max}$), except along $\rho = \rho_{\min}$, since

$$\left(\frac{\partial Z}{\partial T}\right)_{\rho_{\min}=0} = 0$$

4. Since speed of sound values are specified (in the form of F) at pressures calculated from the Peng–Robinson equation of state for the specified set of isotherms and isochores (because true pressures are not known in advance), they are interpolated with respect to pressure using a cubic spline, to pressures from step 1.

5. Having values of compression factor at different densities along each isotherm, partial derivatives

$$\left(\partial Z / \partial \rho\right)_T$$

are estimated from a cubic spline, inside the domain and along the boundary ($T_{\min} \leq T \leq T_{\max}$ and $\rho_{\min} \leq \rho \leq \rho_{\max}$).

6. Specific heat capacities at constant volume are calculated from (7)

$$c_v = \frac{R}{M}\left[Z + T\left(\frac{\partial Z}{\partial T}\right)_\rho\right]^2\left[F - Z - \rho\left(\frac{\partial Z}{\partial \rho}\right)_T\right]^{-1}$$

inside the domain and along the boundary ($T_{\min} \leq T \leq T_{\max}$ and $\rho_{\min} < \rho \leq \rho_{\max}$).

7. Having interpolated values of F to pressures from step 1, values of speed of sound squared are calculated from

$$u^2 = \frac{FRT}{M}$$

8. Having values of density at different pressures along each isotherm, partial derivatives

$$\left(\partial \rho / \partial p\right)_T$$

are estimated from a cubic spline, inside the domain and along the boundary ($T_{\min} \leq T \leq T_{\max}$ and $\rho_{\min} \leq \rho \leq \rho_{\max}$).

9. Specific heat capacities at constant pressure are calculated from (3)

$$c_p = c_v u^2 \left(\frac{\partial \rho}{\partial p}\right)_T$$

inside the domain and along the boundary ($T_{\min} \leq T \leq T_{\max}$ and $\rho_{\min} < \rho \leq \rho_{\max}$).

10. Having values of pressure at different temperatures along each isochore, partial derivatives

$$\left(\partial^2 p / \partial T^2\right)_\rho$$

are estimated from a cubic spline, inside the domain and along the boundary ($T_{\min} \leq T \leq T_{\max}$ and $\rho_{\min} < \rho \leq \rho_{\max}$), except along $\rho = \rho_{\min}$, since

$$\left(\frac{\partial^2 p}{\partial T^2} \right)_{\rho_{\min}=0} = 0$$

Having values of specific heat capacity at constant volume at different densities along each isotherm, partial derivatives

$$\left(\partial c_v / \partial \rho \right)_T$$

are estimated from a cubic spline, inside the domain and along the boundary ($T_{\min} \leq T \leq T_{\max}$ and $\rho_{\min} \leq \rho \leq \rho_{\max}$).

11. Having calculated derivatives in step 10, values of f are calculated from (9)

$$f = -\frac{T}{\rho^2} \left(\frac{\partial^2 p}{\partial T^2} \right)_\rho - \left(\frac{\partial c_v}{\partial \rho} \right)_T$$

inside the domain and along the boundary ($T_{\min} \leq T \leq T_{\max}$ and $\rho_{\min} < \rho \leq \rho_{\max}$), except along $\rho = \rho_{\min} = 0$, because along this isochore, as already stated, the compression factor has unique value 1, and the heat capacities are obtained from speed of sound measurements (extrapolated to zero pressure) directly.

12. Values of f from step 11 are squared (in order to have positive sign) and summed, and the objective function g is then calculated from (10)

$$g = \frac{1}{2} \sum f^2$$

13. If $g > 10^{-4}$, new values of compression factor are calculated using a modified Levenberg–Marquardt algorithm [21], inside the domain ($T_{\min} < T < T_{\max}$ and $\rho_{\min} < \rho < \rho_{\max}$).

14. Steps 1 to 13 are repeated as many times as necessary to find such values of compression factor for which $g \leq 10^{-4}$.

2.2 Subcritical Domain

This domain is bounded by two isotherms, one isochore and the saturation line. In order to make this domain rectangular, density is replaced by quantity $\phi = \rho/\rho_{sat}$. The temperature range is divided into several isotherms and ϕ-range into several lines of constant ϕ. Pressures are calculated along each ϕ again from the Peng–Robinson equation of state, and speed of sound values are specified at these pressures again in the form $F = Mu^2/(RT)$. Initial and boundary values of compression factor are obtained and specified, respectively, as in the case of the supercritical domain.

2.2.1 Algorithm of Solution

1. For the specified set of isotherms and lines of constant ϕ, densities are calculated from (12)

$$\rho = \phi \rho_{sat}$$

   inside the domain ($T_{min} < T < T_{max}$ and $\phi_{min} < \phi < \phi_{max}$).

2. For the specified set of isotherms and densities calculated in step 1, pressures inside the domain ($T_{min} < T < T_{max}$ and $\phi_{min} < \phi < \phi_{max}$) are calculated from compression factors, since they are always known in advance in each iteration. (In the first iteration they are obtained from the boundary values and in all other iterations from a modified Levenberg–Marquardt algorithm.) In any case, this is done by rewriting (6) into

$$p = \frac{\rho R T Z}{M}$$

3. Having values of compression factor at different temperatures along each line of constant ϕ, partial derivatives

$$\left(\partial Z / \partial T \right)_{\phi}$$

   are estimated from a cubic spline, inside the domain and along the boundary ($T_{min} \leq T \leq T_{max}$ and $\phi_{min} < \phi \leq \phi_{max}$), except along $\phi = \phi_{min}$, since

$$\left(\frac{\partial Z}{\partial T} \right)_{\phi_{min}=0} = 0$$

   Having values of compression factor at different densities along each isotherm, partial derivatives

$$\left(\partial Z / \partial \rho \right)_{T}$$

   are estimated from a cubic spline, inside the domain and along the boundary ($T_{min} \leq T \leq T_{max}$ and $\phi_{min} \leq \phi \leq \phi_{max}$).
   Having values of density at different temperatures along line $\phi = 1$ (saturation line), derivatives

$$\mathrm{d} \ln \rho_{sat} / \mathrm{d} T$$

   are estimated from a cubic spline.

4. Partial derivatives of density, with respect to temperature at constant ϕ, are calculated directly from the following relation

$$\left(\frac{\partial \rho}{\partial T} \right)_{\phi} = \phi \rho \frac{\mathrm{d} \ln \rho_{sat}}{\mathrm{d} T}$$

which is obtained by analytical derivation of (12), inside the domain and along the boundary ($T_{\min} \leq T \leq T_{\max}$ and $\phi_{\min} < \phi \leq \phi_{\max}$), except along $\phi = \phi_{\min}$, since

$$\left(\frac{\partial \rho}{\partial T}\right)_{\phi_{\min}=0} = 0$$

5. Partial derivatives of compression factor with respect to temperature at constant density are obtained from those at constant ϕ, according to calculus, as follows

$$\left(\frac{\partial Z}{\partial T}\right)_{\rho} = \left(\frac{\partial Z}{\partial T}\right)_{\phi} - \left(\frac{\partial Z}{\partial \rho}\right)_{T} \left(\frac{\partial \rho}{\partial T}\right)_{\phi}$$

inside the domain and along the boundary ($T_{\min} \leq T \leq T_{\max}$ and $\phi_{\min} < \phi \leq \phi_{\max}$), except along $\phi = \phi_{\min}$, since

$$\left(\frac{\partial Z}{\partial T}\right)_{\rho_{\min}=\phi_{\min}=0} = 0$$

6. For the sake of clarity, it is convenient to introduce new variable a as follows

$$a = \left(\frac{\partial Z}{\partial T}\right)_{\rho}$$

7. Having values of a at different temperatures along each line of constant ϕ, partial derivatives

$$\left(\partial a / \partial T\right)_{\phi}$$

are estimated from a cubic spline, inside the domain and along the boundary ($T_{\min} \leq T \leq T_{\max}$ and $\phi_{\min} < \phi \leq \phi_{\max}$), except along $\phi = \phi_{\min}$, since

$$\left(\frac{\partial a}{\partial T}\right)_{\phi_{\min}=0} = 0$$

Having values of a at different densities along each isotherm, partial derivatives

$$\left(\partial a / \partial \rho\right)_{T}$$

are estimated from a cubic spline, inside the domain and along the boundary ($T_{\min} \leq T \leq T_{\max}$ and $\phi_{\min} \leq \phi \leq \phi_{\max}$).

8. Partial derivatives of a with respect to temperature at constant density are obtained from those at constant ϕ, according to calculus, as follows

$$\left(\frac{\partial a}{\partial T}\right)_{\rho} = \left(\frac{\partial a}{\partial T}\right)_{\phi} - \left(\frac{\partial a}{\partial \rho}\right)_{T} \left(\frac{\partial \rho}{\partial T}\right)_{\phi}$$

inside the domain and along the boundary ($T_{\min} \leq T \leq T_{\max}$ and $\phi_{\min} < \phi \leq \phi_{\max}$), except along $\phi = \phi_{\min}$, since

$$\left(\frac{\partial a}{\partial T}\right)_{\rho_{\min}=\phi_{\min}=0} = 0$$

9. Since speed of sound values are specified (in the form of F) at pressures calculated from the Peng–Robinson equation of state for the specified set of isotherms and lines of constant ϕ (because true pressures are not known in advance), they are interpolated with respect to pressure using a cubic spline, to pressures from step 2.

10. Specific heat capacities at constant volume are calculated from (7)

$$c_v = \frac{R}{M}\left[Z + T\left(\frac{\partial Z}{\partial T}\right)_\rho\right]^2\left[F - Z - \rho\left(\frac{\partial Z}{\partial \rho}\right)_T\right]^{-1}$$

inside the domain and along the boundary ($T_{\min} \leq T \leq T_{\max}$ and $\phi_{\min} < \phi \leq \phi_{\max}$).

11. Having values of compression factor at different pressures along each isotherm, partial derivatives

$$\left(\partial Z / \partial p\right)_T$$

are estimated from a cubic spline, inside the domain and along the boundary ($T_{\min} \leq T \leq T_{\max}$ and $\phi_{\min} \leq \phi \leq \phi_{\max}$).

12. Partial derivatives of density, with respect to pressure at constant temperature, are calculated directly from the following relation

$$\left(\frac{\partial \rho}{\partial p}\right)_T = \frac{M}{ZRT}\left[1 - \frac{p}{Z}\left(\frac{\partial Z}{\partial p}\right)_T\right]$$

which is obtained by analytical derivation of (6), inside the domain and along the boundary ($T_{\min} \leq T \leq T_{\max}$ and $\phi_{\min} \leq \phi \leq \phi_{\max}$).

13. Having interpolated values of F to pressures from step 2, values of speed of sound squared are calculated from

$$u^2 = \frac{FRT}{M}$$

14. Specific heat capacities at constant pressure are calculated from (3)

$$c_p = c_v u^2 \left(\frac{\partial \rho}{\partial p}\right)_T$$

inside the domain and along the boundary ($T_{\min} \leq T \leq T_{\max}$ and $\phi_{\min} < \phi \leq \phi_{\max}$).

15. Having values of specific heat capacity at constant volume at different densities along each isotherm, partial derivatives

$$\left(\partial c_v / \partial \rho\right)_T$$

are estimated from a cubic spline, inside the domain and along the boundary ($T_{\min} \leq T \leq T_{\max}$ and $\phi_{\min} \leq \phi \leq \phi_{\max}$).

16. Having calculated derivatives in steps 5, 8 and 15, values of f are calculated from (17)

$$f = -\frac{RT}{\rho M}\left[2\left(\frac{\partial Z}{\partial T}\right)_\rho + T\left(\frac{\partial a}{\partial T}\right)_\rho\right] - \left(\frac{\partial c_v}{\partial \rho}\right)_T$$

inside the domain and along the boundary ($T_{\min} \leq T \leq T_{\max}$ and $\phi_{\min} < \phi \leq \phi_{\max}$), except along $\phi = \phi_{\min} = 0$, because along this line, as already stated, the compression factor has unique value 1, and the heat capacities are obtained from speed of sound measurements (extrapolated to zero pressure) directly.

17. Values of f from step 16 are squared (in order to have positive sign) and summed, and the objective function g is then calculated from (18)

$$g = \frac{1}{2}\sum f^2$$

18. If $g > 10^{-4}$, new values of compression factor are calculated using a modified Levenberg–Marquardt algorithm [21], inside the domain ($T_{\min} < T < T_{\max}$ and $\phi_{\min} < \phi < \phi_{\max}$).

19. Steps 1 to 18 are repeated as many times as necessary to find such values of compression factor for which $g \leq 10^{-4}$.

3 Results and Discussion

In supercritical domain, a wide range of density/pressure and temperature is covered (see Table 1). The density range exceeds critical point slightly, while temperature range exceeds it several times. The number of isochores, isotherms, speed of sound data points, boundary data points, calculated data points and iterations taken, as well as initial data deviations, is given in Table 3. The speed of sound data points, boundary data points and calculated data points do not include isochore at zero density. The boundary data points consist only of the compression factor and no heat capacities, so the number of calculated heat capacity data points is higher than that of compression factor. The average absolute deviations (AADs) of the calculated data points, with respect to corresponding reference data [18–20], are given in Table 5. Comparison of figures for AAD from Table 3 for initial compression factors (obtained from the boundary values by a cubic spline interpolation with respect to density) and those from Table 5 shows that these last are three orders of magnitude smaller. Since the figures from Table 5 are very small, the results obtained are practically in the limits of experimental uncertainties of corresponding direct measurements. Relative deviations

of calculated data points are presented graphically in Figs. 1, 2, 3, 4, 5 and 6 for argon, Figs. 13, 14, 15, 16, 17 and 18 for methane and Figs. 25, 26, 27, 28, 29 and 30 for carbon dioxide, as a function of density and temperature. From these pictures and graphs, it can be seen that the deviations tend to increase rapidly when approaching the critical point. This happens because derivatives are approximated less accurately in the vicinity of critical point where thermodynamic surface has the highest curvature. This can be mitigated by increasing the number of isotherms in this area. However, it would demand more boundary data points and more equations to be solved.

In subcritical domain, almost a whole range of density/pressure and temperature is covered (see Table 2). The density range includes the saturation line, while temperature range practically extends from triple to critical point. The number of lines with constant ϕ, isotherms, speed of sound data points, boundary data points, calculated data points and iterations taken, as well as initial data deviations, is given in Table 4. The average absolute deviations (AADs) of the calculated data points, with respect to corresponding reference data [18–20], are given in Table 6. Relative deviations of calculated data points are presented graphically in Figs. 7, 8, 9, 10, 11 and 12 for argon, Figs. 19, 20, 21, 22, 23 and 24 for methane and Figs. 31, 32, 33, 34, 35 and 36 for carbon dioxide, as a function of ϕ and temperature.

In order to see how uncertainties in both the boundary conditions and speed of sound data propagate into the final solution, they are perturbed by $\pm 0.1\,\%$, one at a time, and the results obtained are given in Tables 7, 8, 9 and 10. Tables 5 and 6 show that mean AAD of Z without perturbations is $0.0014\,\%$. When the boundary conditions and speed of sound data are perturbed, this figure increases to $0.0910\,\%$ and $0.0041\,\%$, respectively. In the case of c_v, corresponding figures are $0.0320\,\%$, $0.3730\,\%$ and $0.3113\,\%$, and in the case of c_p, they are $0.0572\,\%$, $0.4124\,\%$ and $0.2358\,\%$. Therefore, uncertainties in the boundary conditions have more severe effect on the final solution than those in the speed of sound. However, even these results are still in the limits of experimental uncertainties of direct measurements of corresponding properties, especially having in mind the ρ–T–p ranges covered in both the domains.

4 Conclusions

It is possible to solve the adiabatic sound wave equation in gaseous (vapor) phase as a nonlinear least squares problem, on account of volumetric boundary conditions of Dirichlet type only. When the density range reaches the critical point, the upper limit of temperature range is bounded only by the maximum pressure at which the speed of sound data are available. Although the domain of solution is very wide, the number of equations to be solved is only of the order 10^2, because all the derivatives are obtained from a cubic spline. Accuracy of the results obtained depends on the accuracy of the derivatives estimation, which is in direct correlation with the number of boundary data points. However, this number is rather moderate and experimentally viable, without need for interpolation like in the case of finite differences approximations. This approach is far less sensitive to the accuracy of initial data, in comparison with the numerical integration. It finds solution with AAD of the order 10^{-3} even if initial data AAD is of the order 10^0.

Appendix

See Tables 1, 2, 3, 4, 5, 6, 7, 8, 9 and 10.

Table 1 ρ–T–p ranges covered in supercritical domain

Substance	ρ (kg·m^{-3})		T (K)		p (MPa)	
	Min	Max	Min	Max	Min	Max
Ar	0	550	180	600	0	93.235
CH$_4$	0	180	220	620	0	78.599
CO$_2$	0	500	320	1220	0	165.129

Table 2 ρ–T–p ranges covered in subcritical domain

Substance	ρ (kg·m^{-3})		T (K)		p (MPa)	
	Min	Max	Min	Max	Min	Max
Ar	0	178.858	90	140	0	3.168
CH$_4$	0	61.375	95	180	0	3.285
CO$_2$	0	209.723	220	295	0	5.982

Table 3 Other data for supercritical domain

Substance	ρ, $T=$ const.	u specified	Z, c_v, c_p specified	Z calculated	c_v, c_p calculated	Initial Z AAD (%)	Iterations taken[a]
Ar	12/22	242	42/0/0	200	242/242	4.8173	604
CH$_4$	10/21	180	37/0/0	152	180/180	6.4411	613
CO$_2$	11/46	460	64/0/0	396	460/460	6.1956	1986

[a]With error tolerance 10^{-4}

Table 4 Other data for subcritical domain

Substance	ϕ, $T=$ const.	u specified	Z, c_v, c_p specified	Z calculated	c_v, c_p calculated	Initial Z AAD (%)	Iterations taken[a]
Ar	11/11	110	29/0/0	81	110/110	0.1405	165
CH$_4$	11/18	180	36/0/0	144	180/180	0.1460	291
CO$_2$	11/16	160	34/0/0	126	160/160	0.4301	382

[a]With error tolerance 10^{-4}

Table 5 Average absolute deviation (AAD) in supercritical domain

Substance	AAD (%)		
	Z	c_v	c_p
Ar	0.0018	0.0170	0.0294
CH$_4$	0.0014	0.0165	0.0770
CO$_2$	0.0013	0.0156	0.0466

Table 6 Average absolute deviation (AAD) in subcritical domain

Substance	AAD (%)		
	Z	c_v	c_p
Ar	0.0014	0.0558	0.0608
CH_4	0.0010	0.0260	0.0355
CO_2	0.0012	0.0610	0.0940

Table 7 AAD in supercritical domain when boundary conditions are perturbed + 0.1 %/− 0.1 %

Substance	AAD (%)		
	Z	c_v	c_p
Ar	0.0921/0.0896	0.2508/0.2553	0.3418/0.3589
CH_4	0.0778/0.0765	0.3774/0.3827	0.4585/0.5146
CO_2	0.0821/0.0803	0.3908/0.3896	0.4916/0.5133

Table 8 AAD in subcritical domain when boundary conditions are perturbed + 0.1 %/− 0.1 %

Substance	AAD (%)		
	Z	c_v	c_p
Ar	0.0988/0.0977	0.3554/0.3024	0.3117/0.2824
CH_4	0.0998/0.0988	0.4707/0.4337	0.4157/0.3881
CO_2	0.1000/0.0989	0.4530/0.4138	0.4446/0.4281

Table 9 AAD in supercritical domain when speed of sound data are perturbed + 0.1 %/− 0.1 %

Substance	AAD (%)		
	Z	c_v	c_p
Ar	0.0036/0.0032	0.2089/0.2054	0.1170/0.1201
CH_4	0.0093/0.0085	0.3639/0.3580	0.3041/0.2946
CO_2	0.0073/0.0061	0.4070/0.4090	0.3408/0.3374

Table 10 AAD in subcritical domain when speed of sound data are perturbed + 0.1 %/− 0.1 %

Substance	AAD (%)		
	Z	c_v	c_p
Ar	0.0013/0.0015	0.2020/0.2589	0.1306/0.1610
CH_4	0.0023/0.0021	0.3354/0.3697	0.2580/0.2759
CO_2	0.0019/0.0015	0.2912/0.3262	0.2377/0.2522

Argon in Supercritical Domain

See Figs. 1, 2, 3, 4, 5 and 6.
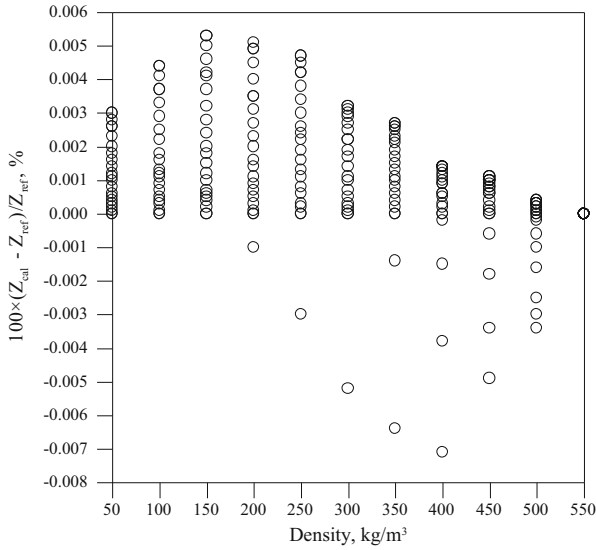
Fig. 1 Relative deviation of Z versus ρ with respect to [18]

Fig. 2 Relative deviation of Z versus T with respect to [18]

Fig. 3 Relative deviation of c_v versus ρ with respect to [18]
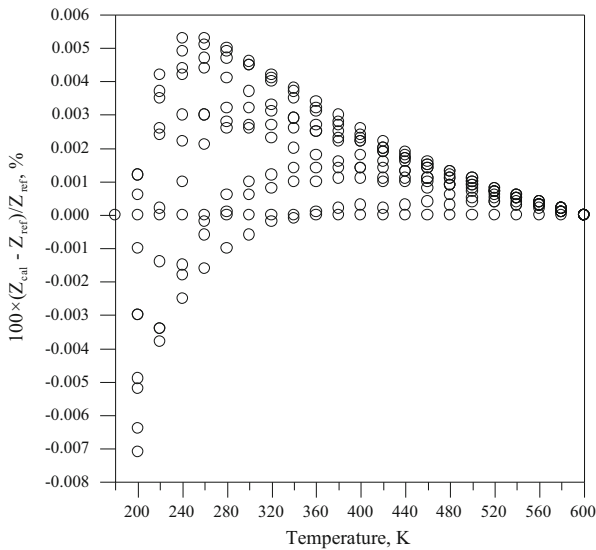
Fig. 4 Relative deviation of c_v versus T with respect to [18]
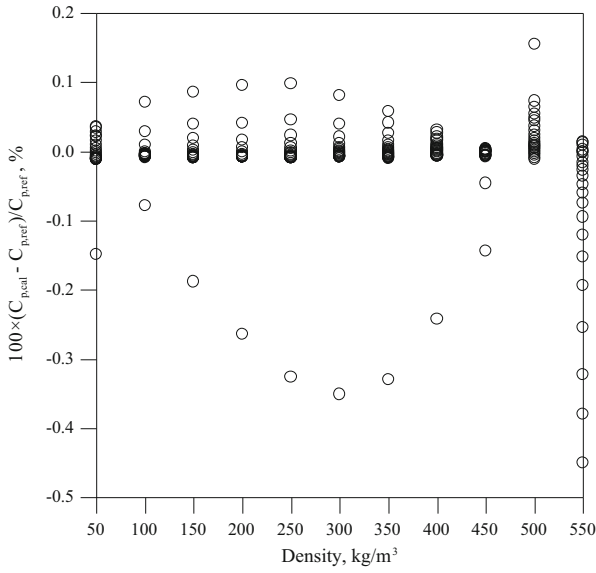
Fig. 5 Relative deviation of c_p versus ρ with respect to [18]
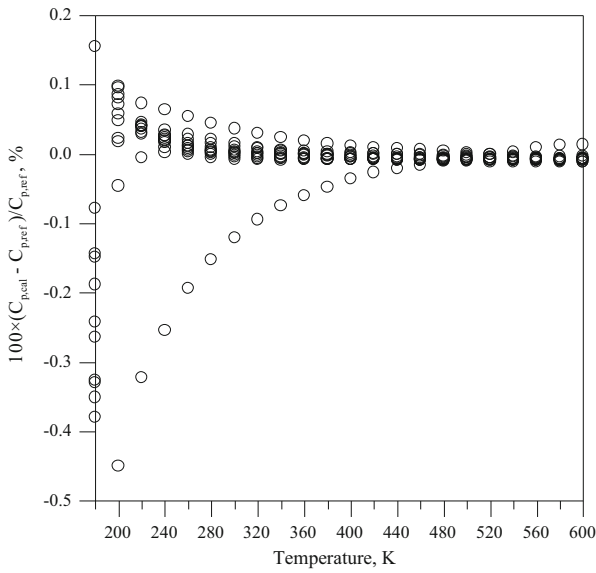
Fig. 6 Relative deviation of c_p versus T with respect to [18]

Argon in Subcritical Domain

See Figs. 7, 8, 9, 10, 11 and 12.
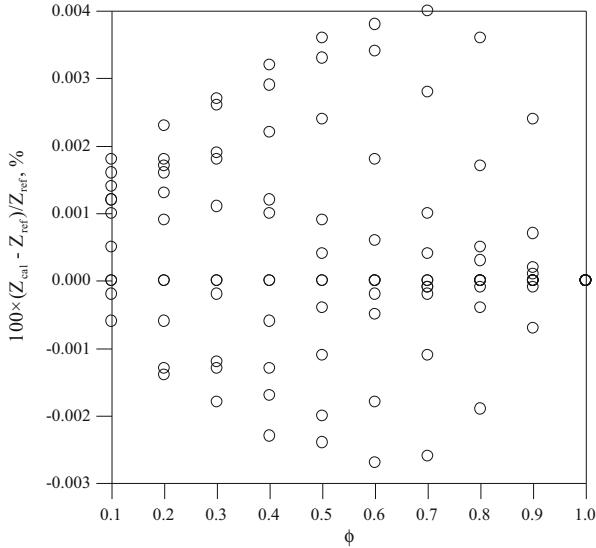
Fig. 7 Relative deviation of Z versus ϕ with respect to [18]
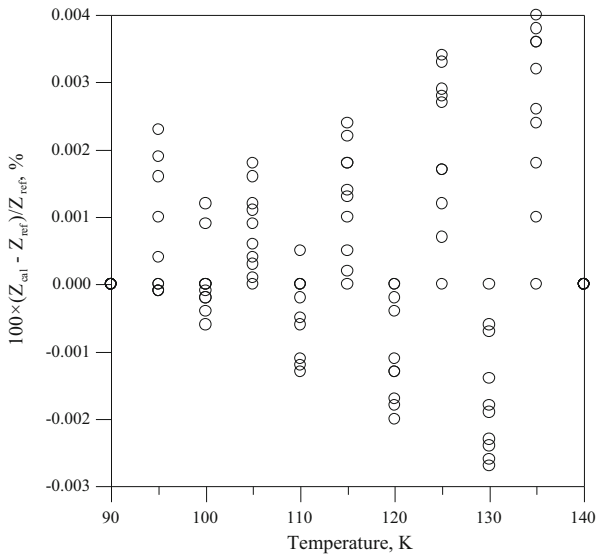
Fig. 8 Relative deviation of Z versus T with respect to [18]
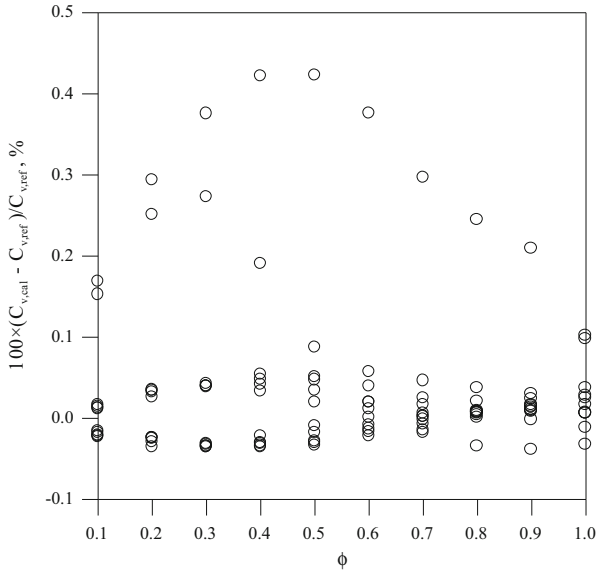
Fig. 9 Relative deviation of c_v versus ϕ with respect to [18]
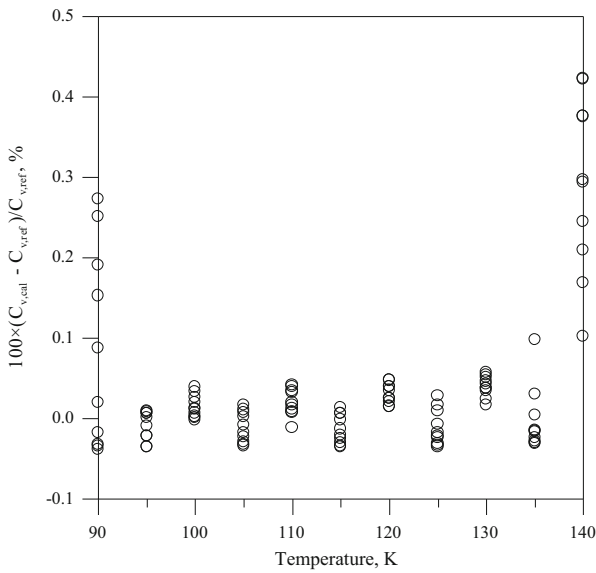
Fig. 10 Relative deviation of c_v versus T with respect to [18]
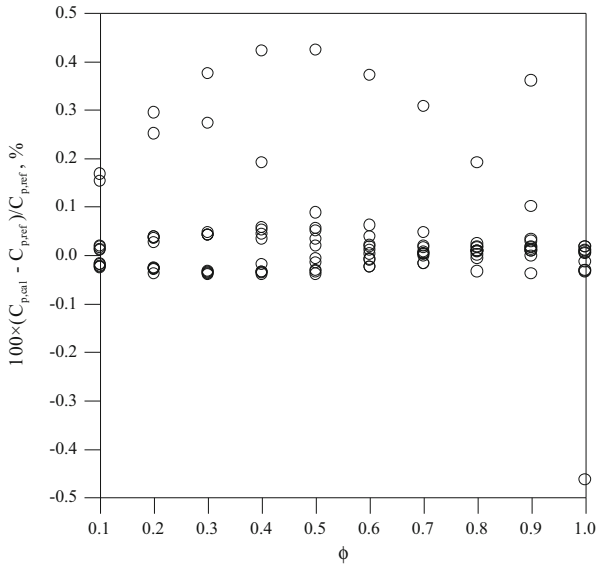
Fig. 11 Relative deviation of c_p versus ϕ with respect to [18]
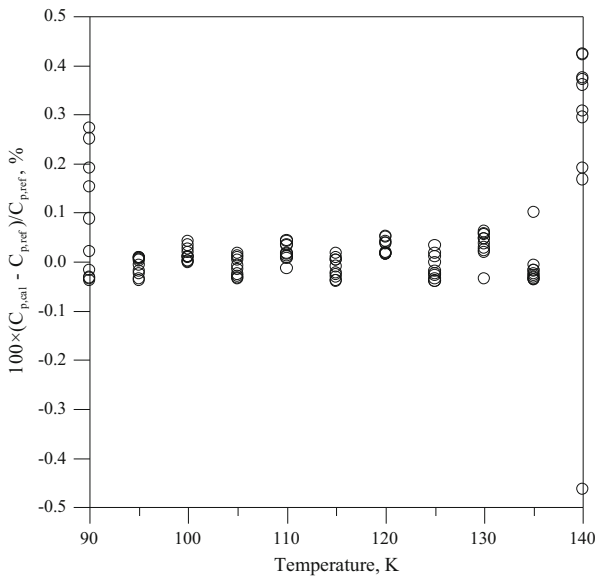
Fig. 12 Relative deviation of c_p versus T with respect to [18]

Methane in Supercritical Domain

See Figs. 13, 14, 15, 16, 17 and 18.
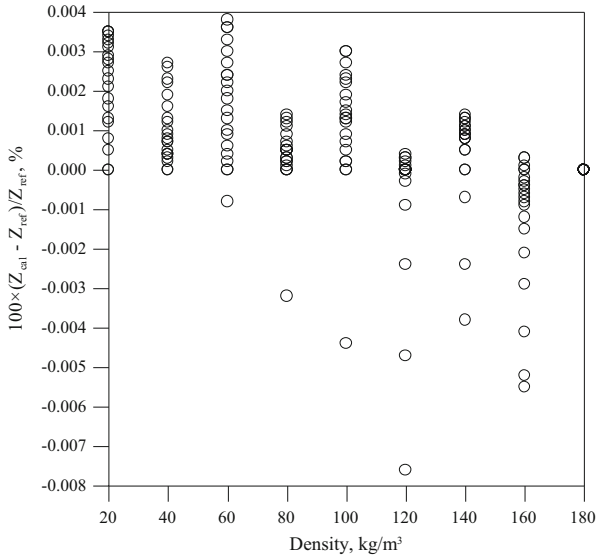
Fig. 13 Relative deviation of Z versus ρ with respect to [19]
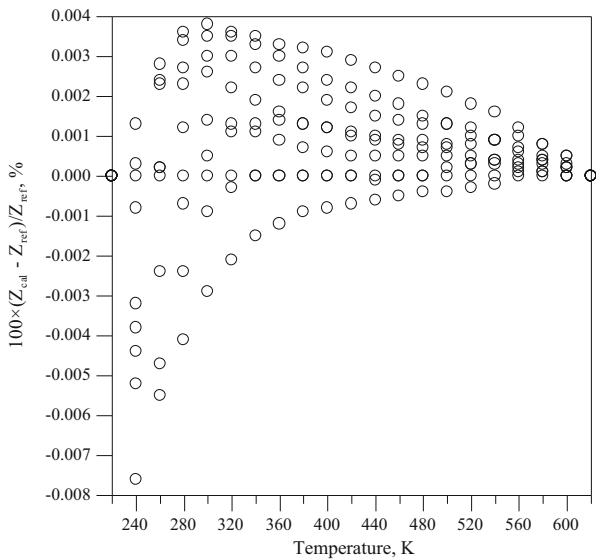
Fig. 14 Relative deviation of Z versus T with respect to [19]
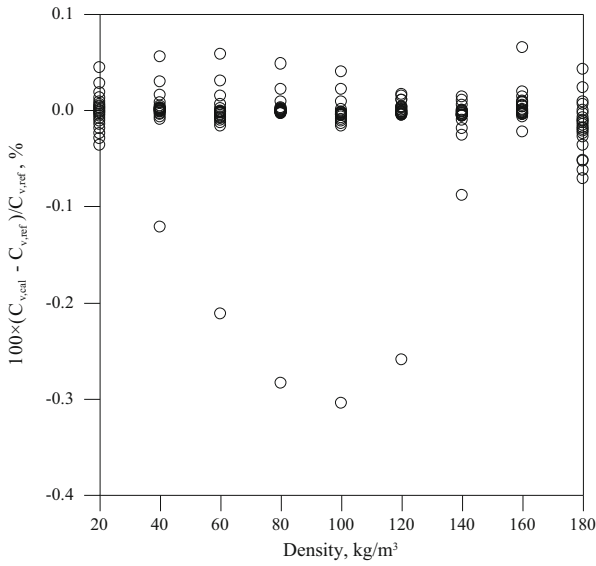
Fig. 15 Relative deviation of c_v versus ρ with respect to [19]
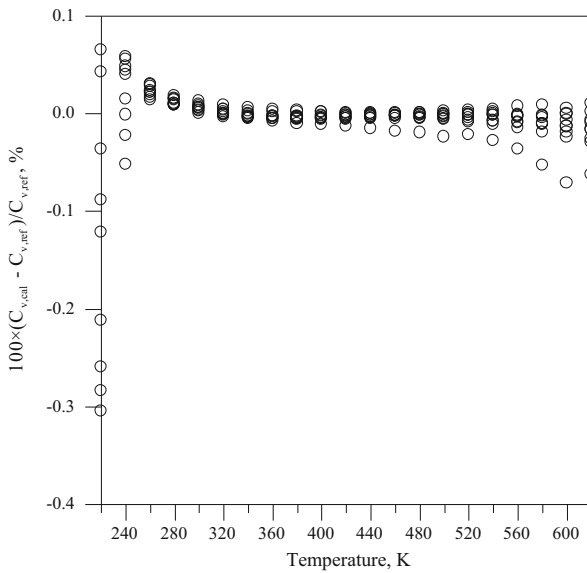
Fig. 16 Relative deviation of c_v versus T with respect to [19]
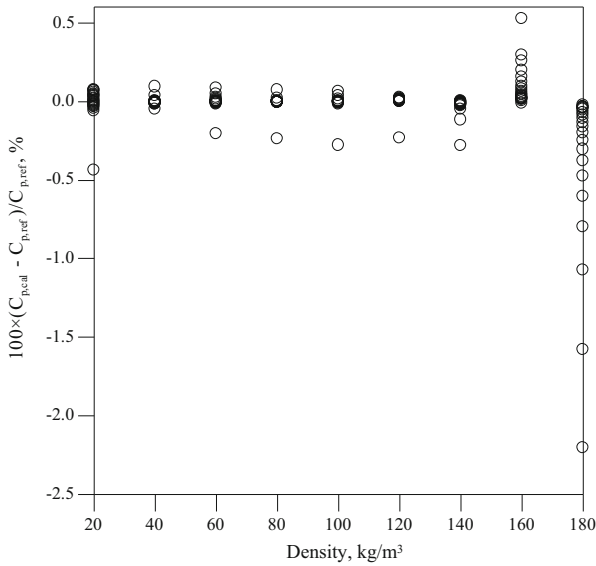
Fig. 17 Relative deviation of c_p versus ρ with respect to [19]
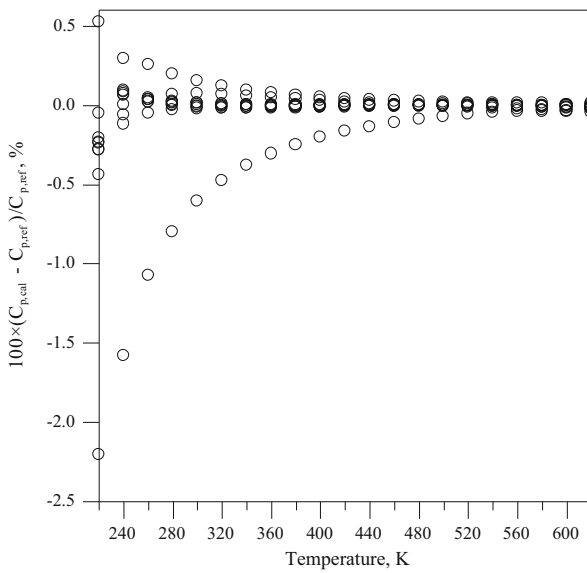
Fig. 18 Relative deviation of c_p versus T with respect to [19]

Methane in Subcritical Domain

See Figs. 19, 20, 21, 22, 23 and 24.
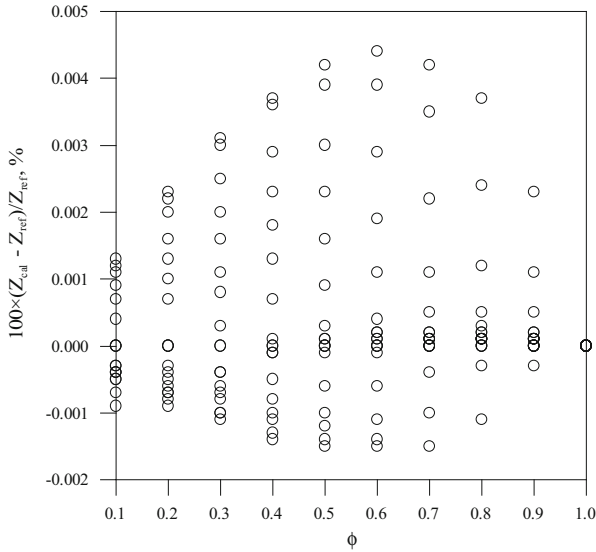
Fig. 19 Relative deviation of Z versus ϕ with respect to [19]
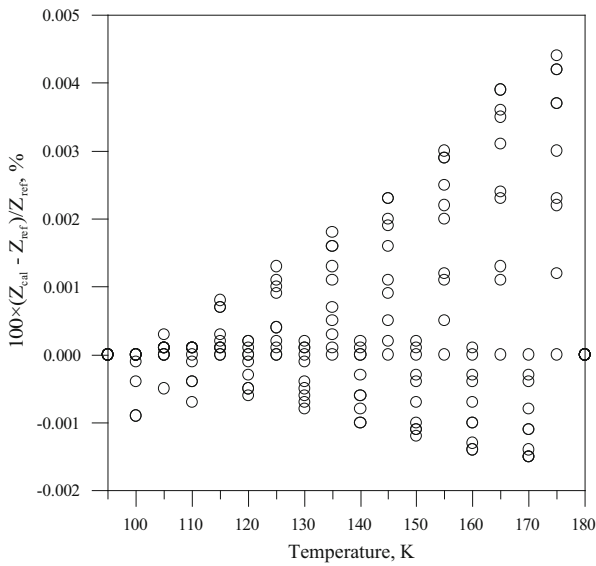
Fig. 20 Relative deviation of Z versus T with respect to [19]
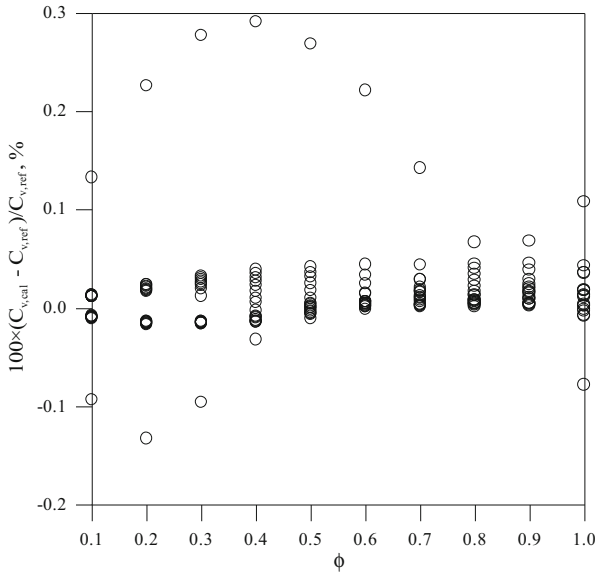
Fig. 21 Relative deviation of c_v versus ϕ with respect to [19]
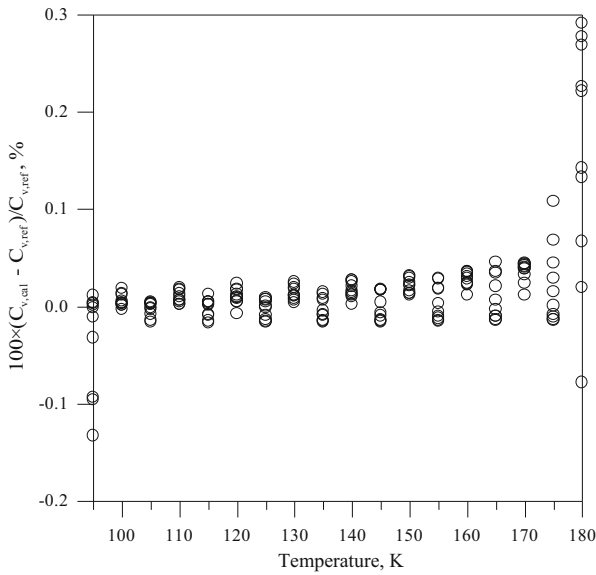
Fig. 22 Relative deviation of c_v versus T with respect to [19]
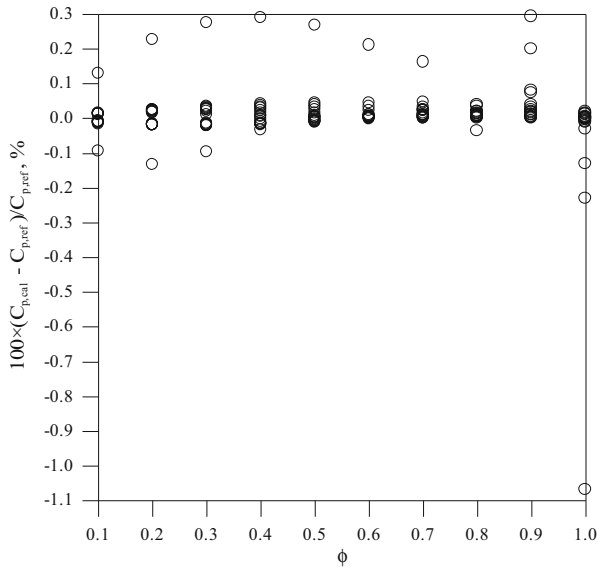
Fig. 23 Relative deviation of c_p versus ϕ with respect to [19]
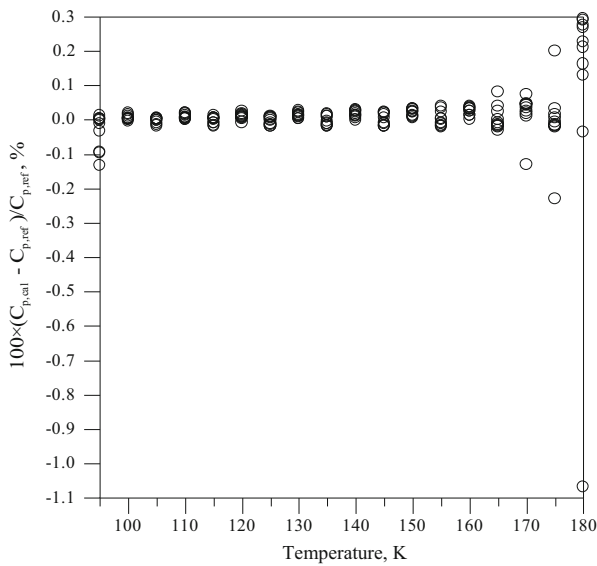
Fig. 24 Relative deviation of c_p versus T with respect to [19]

Carbon Dioxide in Supercritical Domain

See Figs. 25, 26, 27, 28, 29 and 30.
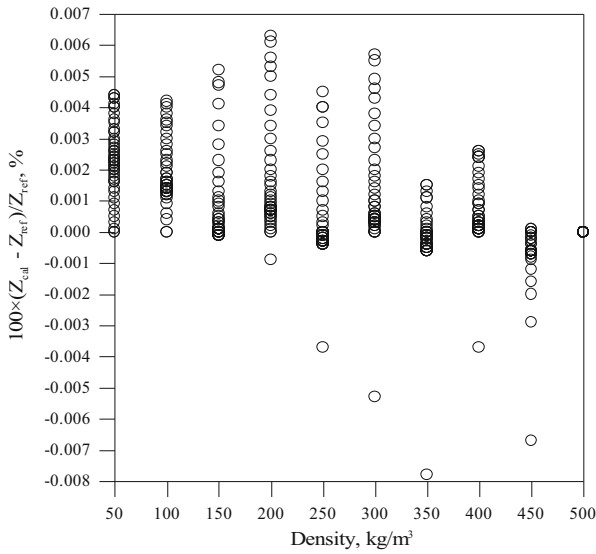
Fig. 25 Relative deviation of Z versus ρ with respect to [20]
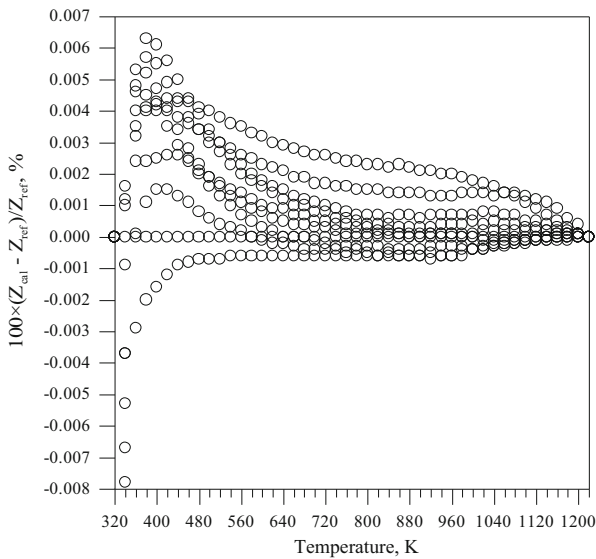
Fig. 26 Relative deviation of Z versus T with respect to [20]
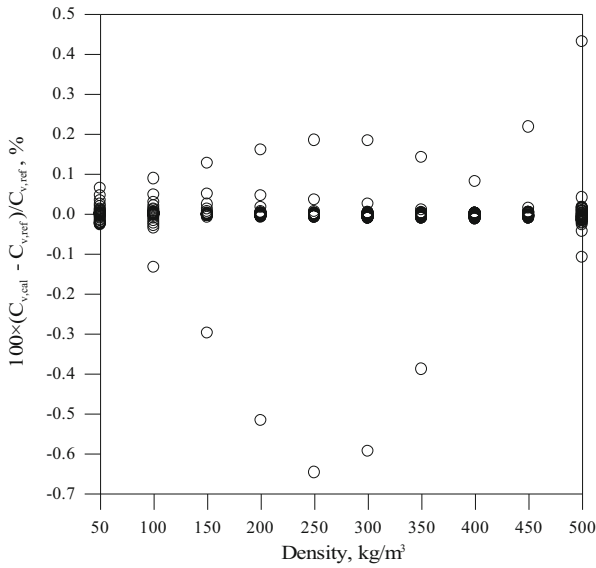
Fig. 27 Relative deviation of c_v versus ρ with respect to [20]
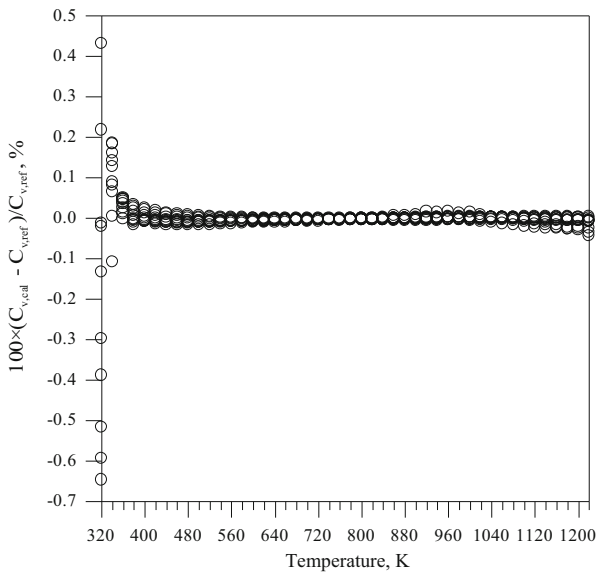
Fig. 28 Relative deviation of c_v versus T with respect to [20]
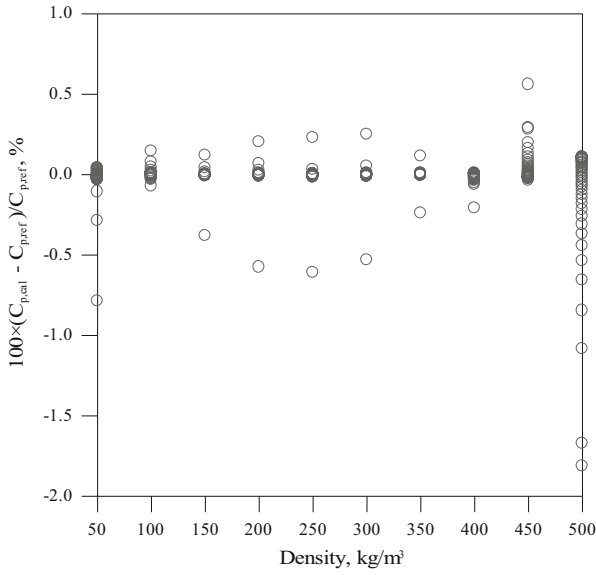
Fig. 29 Relative deviation of c_p versus ρ with respect to [20]
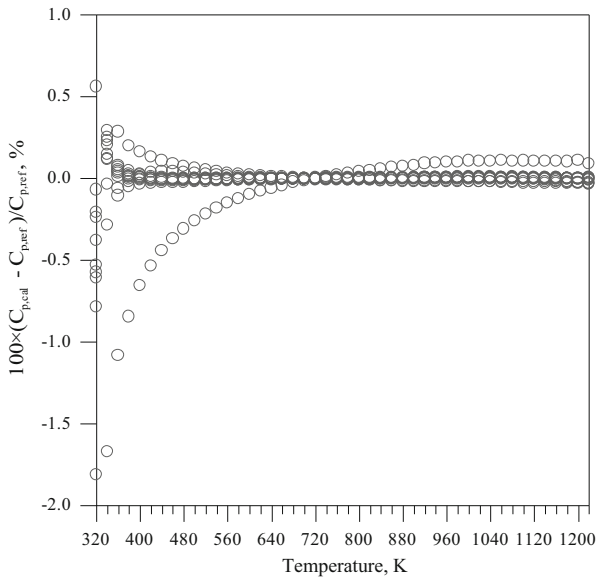
Fig. 30 Relative deviation of c_p versus T with respect to [20]

Carbon Dioxide in Subcritical Domain
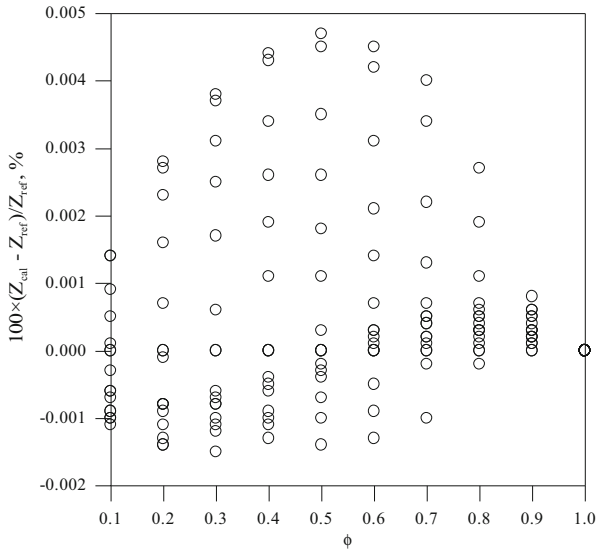
See Figs. 31, 32, 33, 34, 35 and 36.

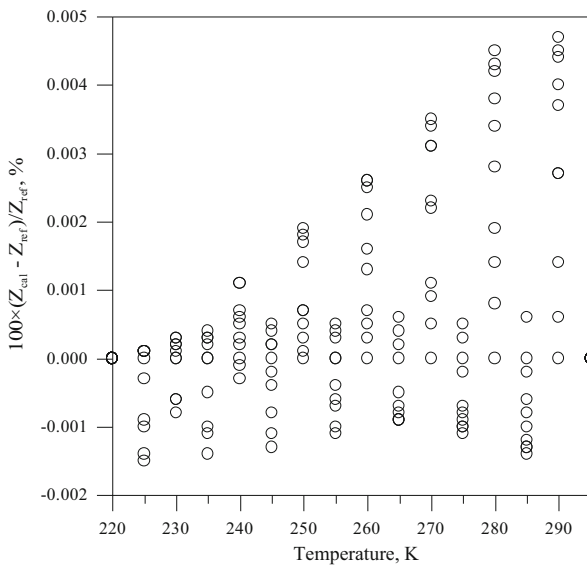**Fig. 31** Relative deviation of Z versus ϕ with respect to [20]

Fig. 32 Relative deviation of Z versus T with respect to [20]
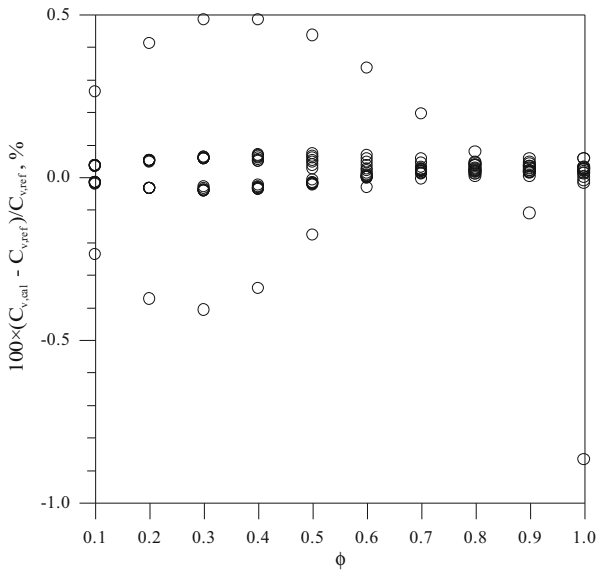
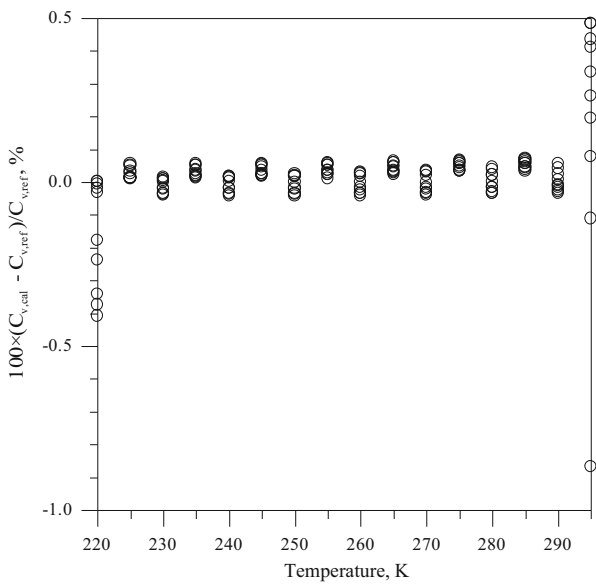**Fig. 33** Relative deviation of c_v versus ϕ with respect to [20]

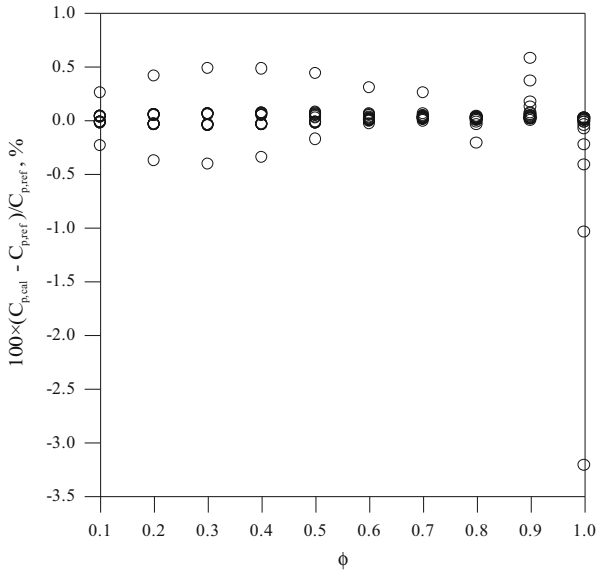**Fig. 34** Relative deviation of c_v versus T with respect to [20]

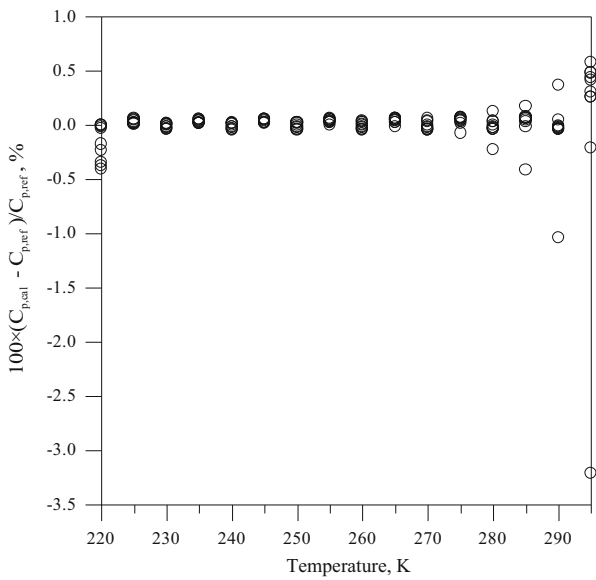**Fig. 35** Relative deviation of c_p versus ϕ with respect to [20]

Fig. 36 Relative deviation of c_p versus T with respect to [20]

References

1. M.J. Moran, H.N. Shapiro, *Fundamentals of Engineering Thermodynamics* (Wiley, Chichester, 2006)
2. J.P.M. Trusler, *Physical Acoustics and Metrology of Fluids* (Adam Hilger, Bristol, 1991)
3. J.P.M. Trusler, M. Zarari, J. Chem. Thermodyn. **24**, 973 (1992)
4. A.F. Estrada-Alexanders, J.P.M. Trusler, M.P. Zarari, Int. J. Thermophys. **16**, 663 (1995)
5. A.F. Estrada-Alexanders, J.P.M. Trusler, Int. J. Thermophys. **17**, 1325 (1996)
6. A.F. Estrada-Alexanders, J.P.M. Trusler, J. Chem. Thermodyn. **29**, 991 (1997)
7. M. Bijedić, N. Neimarlija, Int. J. Thermophys. **28**, 268 (2007)
8. M. Bijedić, N. Neimarlija, J. Iran. Chem. Soc. **5**, 286 (2008)
9. M. Bijedić, N. Neimarlija, Lat. Am. Appl. Res. **43**, 393 (2013)
10. M. Bijedić, S. Begić, J. Thermodyn. **2014**, 1 (2014)
11. A.F. Estrada-Alexanders, D. Justo, J. Chem. Thermodyn. **36**, 419 (2004)
12. C. de Boor, *A Practical Guide to Splines* (Springer, New York, 1978)
13. K. Levenberg, Q. Appl. Math. **2**, 164 (1944)
14. D. Marquardt, SIAM J. Appl. Math. **11**, 431 (1963)
15. J.J. Moré, in *Numerical Analysis, Lecture Notes in Mathematics*, vol. 630, ed. by G.A. Watson (Springer, Berlin, 1978)
16. V.V. Sychev, *The Differential Equations of Thermodynamics* (Mir Publishers, Moscow, 1983)
17. D.Y. Peng, D.B. Robinson, Ind. Eng. Chem. Fundam. **15**, 59 (1976)
18. C. Tegeler, R. Span, W. Wagner, J. Phys. Chem. Ref. Data **28**, 779 (1999)
19. U. Setzmann, W. Wagner, J. Phys. Chem. Ref. Data **20**, 1061 (1991)
20. R. Span, W. Wagner, J. Phys. Chem. Ref. Data **25**, 1509 (1996)
21. J.J. Moré, B.S. Garbow, K.E. Hillstrom, *User Guide for MINPACK-1* (Argonne National Laboratory Report ANL-80-74, 1980)